European Heart Journal Open (2022) **2**, 1–14
https://doi.org/10.1093/ehjopen/oeac018

REVIEW
Cardiac and vascular imaging

Machine learning applications in cardiac computed tomography: a composite systematic review

Jonathan James Hyett Bray [1,2,*], Moghees Ahmad Hanif[2], Mohammad Alradhawi[3], Jacob Ibbetson[2], Surinder Singh Dosanjh[3], Sabrina Lucy Smith[4], Mahmood Ahmad [2,3], and Dominic Pimenta [5]

[1]Institute of Life Sciences 2, Swansea University Medical, School, Swansea, UK; [2]Cardiology Department, Royal Free Hospital, Royal Free London NHS Foundation Trust, London, UK; [3]University College London Medical School, London WC1E 6DE, UK; [4]Barts and the London School of Medicine and Dentistry, London E1 2AD, UK; and [5]Richmond Research Institute, St George's Hospital, University of London, Cranmer Terrace, Tooting, London SW17 0RE, UK

Received 8 January 2022; revised 10 March 2022; online publish-ahead-of-print 17 March 2022

Handling Editor: Alessia Gimelli

Artificial intelligence and machine learning (ML) models are rapidly being applied to the analysis of cardiac computed tomography (CT). We sought to provide an overview of the contemporary advances brought about by the combination of ML and cardiac CT. Six searches were performed in Medline, Embase, and the Cochrane Library up to November 2021 for (i) CT-fractional flow reserve (CT-FFR), (ii) atrial fibrillation (AF), (iii) aortic stenosis, (iv) plaque characterization, (v) fat quantification, and (vi) coronary artery calcium score. We included 57 studies pertaining to the aforementioned topics. Non-invasive CT-FFR can accurately be estimated using ML algorithms and has the potential to reduce the requirement for invasive angiography. Coronary artery calcification and non-calcified coronary lesions can now be automatically and accurately calculated. Epicardial adipose tissue can also be automatically, accurately, and rapidly quantified. Effective ML algorithms have been developed to streamline and optimize the safety of aortic annular measurements to facilitate pre-transcatheter aortic valve replacement valve selection. Within electrophysiology, the left atrium (LA) can be segmented and resultant LA volumes have contributed to accurate predictions of post-ablation recurrence of AF. In this review, we discuss the latest studies and evolving techniques of ML and cardiac CT.

* Corresponding author. Email: jonathanjhbray@gmail.com

Graphical Abstract

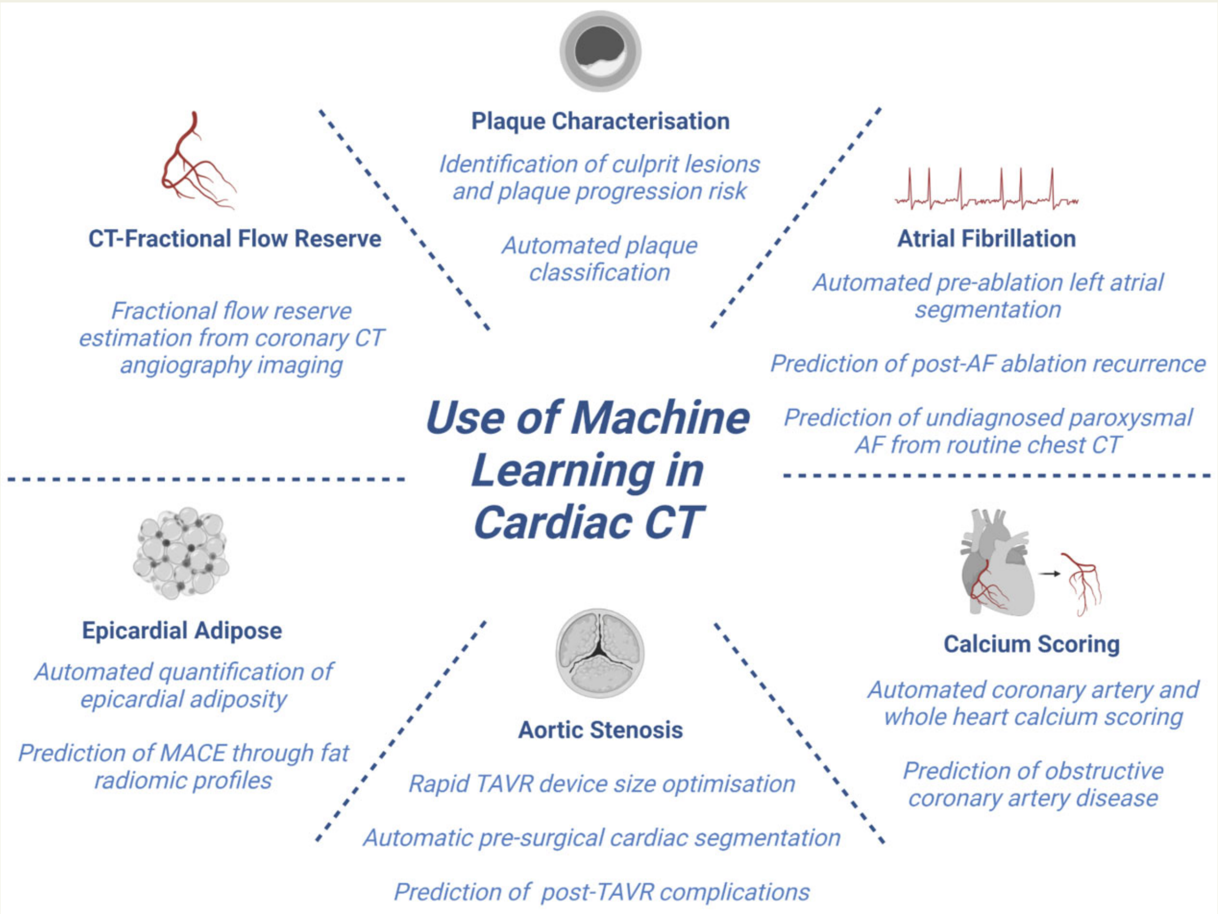

Keywords Machine learning • Artificial intelligence • Cardiac computed tomography

Introduction

Recent advancements in computed tomography (CT) and data science have fostered the development of machine learning models across several domains within cardiology. Clinical implementation of dual-energy CT systems has improved diagnostic accuracy, reduced calcium blooming artefact, enabled identification of atherosclerotic plaque composition, and decreased the radiation and contrast required for scans, while also paving the way for the identification of novel imaging biomarkers and radiomic profiles.[1] New 256- and 320-slice CT systems significantly reduce radiation doses by achieving a full volume acquisition in one to two cardiac cycles. This reduces cardiac motion artefact, improves image quality and diagnostic accuracy, and enables better quantitative analysis.[2] These newer systems are relatively expensive and further research is needed into their full potential. In this review, we provide an up-to-date summary of the evolving machine learning (ML) techniques used in conjunction with cardiac CTs, including: (i) coronary artery imaging [fractional flow reserve (FFR), coronary artery calcium (CAC), and plaque characterization], (ii) epicardial adiposity quantification, (iii) aortic stenosis (AS), and (iv) atrial fibrillation (AF).

Terminology

A paucity of universally accepted terms and the relationships between ML and other aspects of artificial intelligence (AI) can lead to misunderstanding. Artificial intelligence is an umbrella term given to any algorithm mimicking a human being's method of problem-solving. Machine learning falls under this category by using probability and statistics to make predictions based on data. *Table 1* shows examples of specific tools used. The process of ML starts with patient data and finishes with a final prediction as follows: (i) data collection, (ii) pre-processing, (iii) application of the ML algorithm, and (iv) optimization of the aforementioned steps. Machine learning algorithms can be further classified based on whether they require input 'training data' that comprises the original patient data and a corresponding data class 'label'. The volume and quality of

Table 1 An overview of algorithms used in machine learning with summary definitions and benefits

Algorithm	Overview
Logistic regression	Determines the probability of a particular class for a discrete variable. A simple algorithm with extensive applications.
Support vector machines	Uses 'kernel mapping' to set boundaries of data classes. Can be used for hand-written characters and text categorization but is limited in larger datasets.
k-nearest neighbour	Classifies data based on the classes of the *k* closest data points (where *k* is a positive, whole number). Simple and easy to implement.
Random forest	A collection of decision trees that iteratively split data based on binary criteria. The output is a combination of the results of each single decision tree. A major advantage is its ability to prioritize more important characteristics of the dataset. A highly versatile classifier that works well with small datasets.
Convolutional neural networks (U-Net)	A convolutional neural network (CNN) is a deep learning algorithm that captures the essence of data using a filter based on convolution. This is used extensively in image processing applications. U-net is a specific form of CNN architecture that utilizes fewer training images to provide more accurate segmentation.[3]

'training data', in combination with the appropriateness of the statistical algorithm applied, correlates with the utility of an ML model. Algorithms that require 'training data' are termed 'supervised learning' algorithms and are discussed in this review; in contrast to 'unsupervised learning' that do not require 'training data'.

Methods

We performed six searches of Medline, Embase, and the Cochrane Library up to November 2021 for original articles containing human subjects pertaining to the use of ML in (i) CT-fractional flow reserve (CT-FFR), (ii) AF, (iii) AS, (iv) plaque characterization, (v) fat quantification, and (vi) CAC score (*Figure 1*). The following terms were used, including MeSH terms, synonyms, and abbreviations (CAC score/ fractional flow reserve/ atrial fibrillation/ aortic stenosis/ coronary plaque/ fat quantification) AND (machine learning OR neural network OR *k*-nearest neighbour OR random forest) AND (computer tomography). Studies utilizing deep learning algorithms other than convolutional neural network (CNN) were excluded. Duplicates were removed from each search, before titles and abstracts were screened by two authors for each search. Studies were selected if they were original articles describing the use of ML and cardiac CT in each topic. Articles identified are summarized in *Tables 2–7*.

Applications of machine learning in cardiac computed tomography

CT-fractional flow reserve

The degree of stenosis on coronary CT angiography (CCTA) does not always correlate with functional flow restriction. For stable coronary artery disease (CAD) invasive physiological assessment using FFR or instantaneous wave-free ratio (iFR) remains the invasive gold standard in assessing flow-limiting lesions, with an FFR $\leq$ 0.8 or iFR $\leq$ 0.89 suggesting the need for follow on percutaneous coronary intervention. Advancements in computational fluid dynamics have allowed for the estimation of FFR from CCTA imaging data, resulting in the development of CT-FFR protocols.

Using numerous iterations of CNN algorithms, CT-FFR has consistently been demonstrated to be superior to CCTA in assessing flow-limiting lesions with an average area under the curve (AUC) of 0.89 (*Table 2*).[6,8,11–15] Early work demonstrated that this technique can reduce processing durations by 80-fold compared with physics-based computations,[5] in addition to being less computationally demanding.[6] Nevertheless, Itu *et al.*[5] was trained on synthetic phantoms and thus lack certain physiological traits that may detrimentally affect clinical accuracy.[5] Moreover, the study by Xu *et al.*[8] demonstrated the effect of poor image quality and tachycardia on the performance of the algorithm. Indeed, performance was substantially decreased in low-quality images vs. high-quality images, subjectively determined by expert readers (AUC: 0.80 vs. 0.93, respectively).[8] Moreover, in a multicentre study by Tesche *et al.*[14], performance was also impacted by the CAC burden. Performance of CT-FFR, per vessel, was significantly affected at higher Agatston scores. This appeared to be due to a negative dose–response effect on specificity with higher CAC scores.[14] In 2021, The National Institute for Health and Care Excellence updated its guidance recommending the use of CT-FFR_{ML}, provided by companies such as HeartFlow, as it is non-invasive, considered to deliver high diagnostic accuracy, whilst having the potential to be cost-effective.[63] In conjunction, contemporary American and European guidelines also support the use of CT-FFR_{ML}.[64,65]

Calcium scoring

Coronary artery calcium predicts cardiovascular events.[66] Low dose electrocardiogram-gated non-contrast CT imaging (CCT) is an effective and non-invasive way for quantifying CAC, having a high sensitivity and negative predictive value for obstructive CAD.[67] Coronary artery calcium is traditionally measured in Agatston scores, which grade calcium severity by multiplying the area of calcification by CT attenuation in Hounsfield units yielding an estimated total CAC burden.[67] Agatston scores correspond to calcification burden, as so: 1–100 mild; 101–400 moderate; and >400 severe.[68]

Machine learning has been used for the automation of CAC identification and scoring with subsequent risk categorization of CAD or future cardiac events; easing the burden on reporting clinicians thereby saving both time and resources (*Table 3*). The use of gradient boosting algorithms has had success in predicting prognosis for patients with suspected cardiovascular disease. In a large retrospective cohort by Nakanishi *et al.*,[20] ML-derived predictions with combined

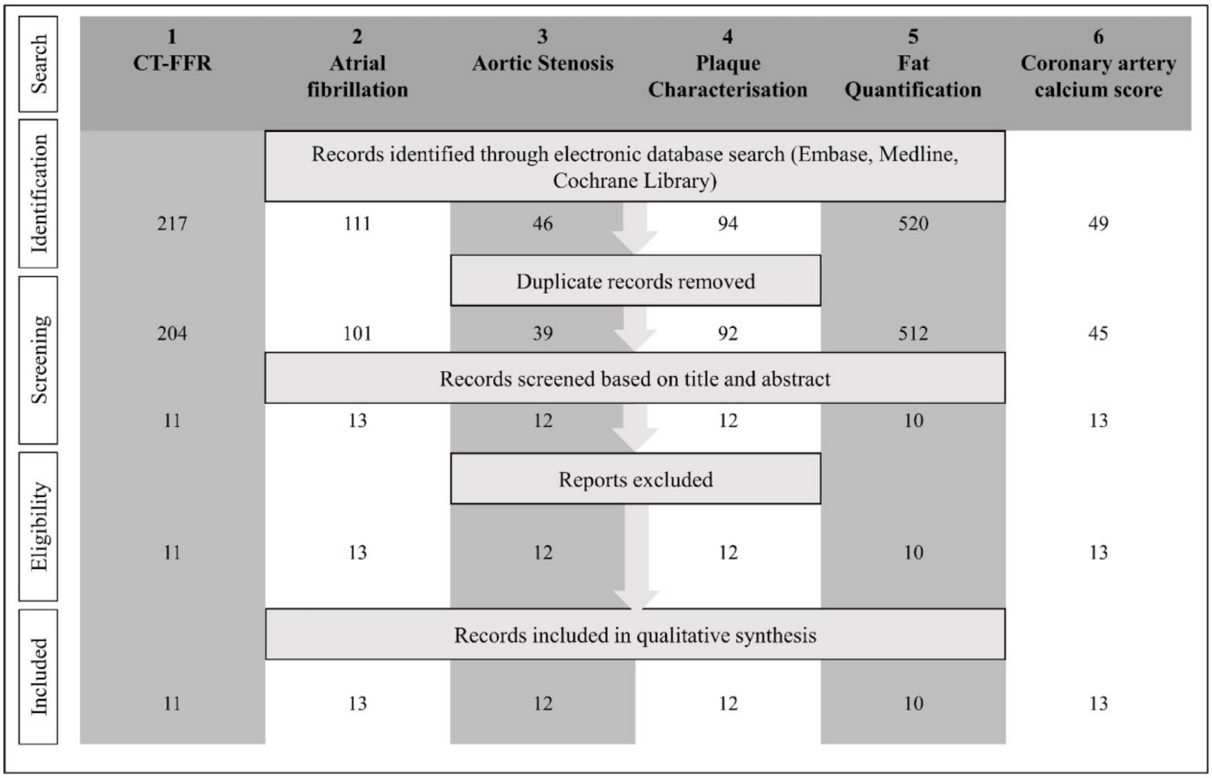

Figure 1 Flow diagram based on PRISMA (preferred reporting items for systematic reviews and meta-analyses) checklist[4] showing resulting articles found and reasons for exclusion.

data were superior to (i) clinical data, (ii) CAC score, and (iii) CT variables alone. This was consistent with Commandeur *et al.*[23], who performed prospective analysis of 1912 individuals and found ML-derived predictions to be superior to traditional atherosclerotic cardiovascular disease risk algorithm and CAC score. These predictive ML algorithms also predict obstructive CAD with a high degree of accuracy (AUC: 0.77;[24] sensitivity: 100 $\pm$ 0.0% and specificity 69.8 $\pm$ 3.6%[25]). Automated identification of CAC score has been performed using *k*-nearest neighbour, CNN and gradient boosting ML with reasonably good accuracies (sensitivity: 73.8% and false positive rate: 0.1 errors per scan;[16] sensitivity: up to 72% and false positive rate: as low as 0.48 errors per scan;[18] and AUC: 0.67–0.85,[19] respectively). It has also been proposed that CAC score can be predicted from clinical variables.[26]

CCT-based, whole heart and vessel-specific CAC scoring algorithms have been developed to include Agatston, mass, and volume scores.[17] They use a *k*-nearest number classifier with forward feature selection on vessels identified from an atlas-based approach with relatively high degrees of sensitivity and low false-positive rates.[17] Similar vessel-specific volume-based CAC scores were achieved in another study using random forest algorithms with fuzzy spatial features to achieve total intraclass correlation coefficients of 0.99 and an accuracy of 1.0 κ in risk class assignment, at a 10 s run time.[21] Lossau *et al.*[22] have developed CNN trained on simulated cardiac motion images, aimed to automate the estimation and correction of coronary motion in coronary computed tomographic angiography (CCTA) scans, with small degrees of error. This approach may be useful in the CCTA calculation of CAC; however, the results were based on a small dataset of 12 clinical cases.

Plaque characterization

Nine studies were identified pertaining to plaque characterization by cardiac CT and the use of ML (*Table 4*). Earlier studies demonstrated that non-calcified plaques could be identified using ML, with extreme gradient boosting algorithms[29] proving superior to topological soft-gradient detection methods[27] (AUC 0.92 vs. 0.87, respectively). Masuda *et al.*[29] also showed that their algorithmic approach performed better than the median CT number. Validated methods of ascertaining morphological characteristics of plaques using ensemble methods and multi-task CNNs have been produced.[6,28] Using similar boosted ensemble algorithms, studies have managed to identify culprit stenotic lesions, predict individuals at risk of rapid coronary plaque progression, and retrospectively predict individuals at risk of major adverse cardiovascular events (MACE), with high degrees of accuracy (AUC: 0.77; 0.83; and 0.96, respectively).[29,31,32] The CAD reporting and data system is designed to classify severely obstructed coronary lesions on CCTA. Muscogiuri *et al.*[33] have demonstrated that a deep learning CNN algorithm can classify over 5 times faster than expert readers, although with an accuracy of between 60% and 86%. It has also been demonstrated that analysis of plaque characteristics can predict MACE[34] and other clinically relevant composite

Table 2 Summary of articles investigating the use of CT-fractional flow reserve using machine learning (CT-FFR_{ML})

Study	Design and aim	Algorithm used	Participants	Outcome
Itu 2016[5]	*In vitro*-validated, *in vivo*-tested, diagnostic accuracy comparison of CT-FFR_{ML} vs. invasive FFR and CT-FFR_{CFD}	CNN	87	AUC: 0.90 Accuracy: 83.2% Sensitivity: 81.6% Specificity: 83.9% PPV: 68.9% NPV: 91.2% Time: 2.4 s
Coenen 2018[6]	Multicentre, retrospective, diagnostic accuracy comparison of CT-FFR_{ML} vs. invasive CCTA and CT-FFR_{CFD}	CNN	351	AUC: 0.84 Accuracy: 85% Sensitivity: 77% Specificity: 89% PPV: 76% NPV: 89%
Tesche 2018[7]	Single-centre, retrospective, diagnostic accuracy comparison of CT-FFR_{ML} vs. CT-FFR_{CFD} and QCA	CNN	85	AUC: 0.91 Sensitivity: 90% Specificity: 95% PPV: 90% NPV: 95% Time: 40.5 min
Xu 2020[8]	Investigation of the impact of image quality, BMI, sex, HR, and calcium on CT-FFR_{ML} diagnostic accuracy vs. CCTA and invasive FFR	-	437	AUC, LQ: 0.80 HQ: 0.93 Accuracy, LQ: 83% HQ: 94% Sensitivity, LQ: 78% HQ: 84% Specificity, LQ: 86% HQ: 98% PPV, LQ: 82% HQ: 95% NPV, LQ: 83% HQ: 93%
Zreik 2020[9]	Retrospective study investigating automatic calculation of CT-FFR (FFR cut off <0.9)	CNN	187	AUC: 0.87 Accuracy: 80%
Baumann 2020[10]	Single-centre, retrospective, diagnostic accuracy comparison of CT-FFR_{ML} vs. iFR	CNN	40	AUC: 0.96 Accuracy: 95% Sensitivity: 92% Specificity: 96% PPV: 92% NPV: 96% Time: 11 min
Lossnitzer 2020[11]	Single-centre, retrospective, diagnostic accuracy comparison of CT-FFR_{ML} vs. invasive FFR and CCTA	CNN	88	AUC: 0.96 Sensitivity: 93% Specificity: 94% PPV: 93% NPV: 94% Time: 23.9 min
Li 2021[12]	Single-centre, retrospective, diagnostic accuracy comparison of CT-FFR_{ML} vs. invasive FFR and CCTA	CNN	73	CT-FFR vs. CCTA vessel-level AUC: 0.957 vs. 0.599, $P < 0.0001$ Accuracy: 90.4% Sensitivity: 93.6% Specificity: 88.1% PPV: 85.3% NPV: 94.9%
Morais 2021[13]	Single-centre, retrospective, diagnostic accuracy comparison of CT-FFR_{ML} vs. invasive FFR	CNN	93	AUC: 0.93 Sensitivity: 87%

Continued

Table 2 ***Continued***

Study	Design and aim	Algorithm used	Participants	Outcome
				Specificity: 86% PPV: 73% NPV: 94%
Renker 2021[14, 15]	Multicentre, retrospective *post hoc* per-vessel diagnostic accuracy analysis of MACHINE registry comparing of CT-FFR_{ML} vs. invasive FFR and CCTA	CNN	330	Overall average (LAD, LCx and RCA) AUC: 0.784 Sensitivity: 78.4% Specificity: 77.2% PPV: 64.7% NPV: 86.6%

Time is reported as an approximation of total time required for analysis. Statistics are per patient (per vessel).
AUC, area under the curve; CFD, computational fluid dynamics; CNN, convolutional neural networks; HR, heart rate; HQ, high-quality images; LQ, low-quality images; low Agatston score, >0 to <100; high Agatston score, >400; QCA, quantitative coronary angiography; iFR, instantaneous wave-free ratio.

outcomes[35] with high degrees of accuracy (AUC: 0.96 and 0.797, respectively).

Epicardial adipose tissue quantification

The epicardial adipose tissue (EAT), being the fat contained between the pericardium and surface of the myocardium, is involved in a complex interplay with the coronary arteries. It is thought that dysfunctional pro-inflammatory adipokines mediate the development of an elevated risk of CAD and MACE.[69] Another effective use of ML in the analysis of cardiac CT output is in the fully-automated identification and quantification of EAT. Studies have done this using numerous algorithmic approaches (*Table 5*), achieving accuracies up to 98.5%,[36] with excellent correlation with expert readers (Pearson's correlation, $r > 0.924$),[37–40,42] and almost identical intra-study dice similarity coefficients (DSCs).[36,39,43,44] A similar technique has been used in combination with a fat radiomic profile (FRP) derived from biopsy and CCTA data of perivascular adipose tissue in a retrospective study by Oikonomou *et al.*[41] to predict MACE at a 5-year follow-up superior to traditional risk stratification tools with an AUC of 0.880 with FRP and an AUC of 0.754 without FRP.

Aortic stenosis

Transcatheter aortic valve replacement (TAVR) is a successful percutaneous intervention for the treatment of severe AS, that is increasingly being used in lower surgical-risk patients.[70] For successful deployment of a TAVR device, pre-operative CT imaging is used to derive various anatomical features of the aortic valve to guide optimal device size selection in order to limit paravalvular regurgitation, coronary obstruction, and conduction disturbance.[47,71] Automated segmentation of the aortic annulus perimeter has been reported using several methods (*Table 6*). Elattar *et al.*[47] developed a method using thresholding, morphological operators, and fuzzy classification to achieve identical DSC coefficients (0.95 vs. 0.95) at over 13-times faster-processing speeds vs. expert reader. This method, however, did not perform segmentation of the valve leaflets themselves. Al *et al.*[49] developed a bespoke regression tree-based algorithm to localize all eight aortic valve landmarks required for pre-operative assessment of TAVR procedures, yielding a mean localization error of 2.04 mm and a run time of 12 ms compared with an inter-observer variability of 2.38 mm. To enable segmentation of aortic valve landmarks, Al Abdullah *et al.*[49] developed a regression tree-based algorithm, yielding high accuracies (mean localization error: 2.38 mm), fast run times (12 ms), and close comparability to expert readers (inter-observer variability: 2.38 mm). Moreover, this model was trained on a generalizable population of patients with variable valvular calcification.[49] To address the computational modelling of valve biomechanics, Liang *et al.*[48] developed a novel method utilizing CT imaging for the reconstruction of 3D valve geometries with built in mesh correspondence. This approach used linear coding and shape dictionary learning based on *k*-nearest number algorithms to achieve patient-specific reconstructions with mean discrepancies of 1.57 mm. A limitation of this study was the lack of patients with severe AS, and thus it lacks the impact of valvular calcification on valvular biomechanics.[48] More recently, in a small number of patients with hypertrophic obstructive cardiomyopathy undergoing surgery, CNN models have been used to automatically segment the cardiac structure.[55] This cut time required down from 3 h manually segmenting to 5 min, although one of the two cases did require some manual adjustment.[55]

As mortality following TAVR can vary widely, ML can also be used to predict post-procedural survival and thus identify individuals who are likely to benefit from the intervention. Using Gradient boosting ML and Cox proportional hazard regression models, it has been possible to predict survival to an AUC of 0.72–0.79,[52,54] is superior to manual scoring systems (TAVI2-SCORE: 0.56 and CoreValve Score: 0.53),[52] and the predictive capacity appears to persist up to 5 years.[54]

Atrial fibrillation

Computed tomography imaging is used in pre-operative mapping prior to ablation for AF to assess left atrium (LA) chamber size and pulmonary vein (PV) anatomy. However, the task of isolating the LA and deriving volumes manually is time-consuming. Studies

Table 3 Summary of studies investigating the use of ML, cardiac CT, and CAC score

Study	Design and aim	Algorithm used	Participants	Outcome
Išgum 2007[16]	Accurate, automated identification of CAC scores	*k*-nearest neighbour and feature selection scheme	76 female participants	Sensitivity 73.8% False-positive rate: 0.1 errors per scan
Shahzad 2013[17]	Automatic detection of whole heart calcium lesions, at 1.5 and 3.0 mm slice spacing	*k*-nearest neighbour	366 patients (training 57%, testing 43%)	• 1.5 mm sensitivity: 81.2% • 1.5 mm false positive rate: 2.5 errors per patient • 3.0 mm sensitivity: 86.6% • False-positive rate: 2.2 errors per patient
Wolterink 2016[18]	Accurate, automated identification of CAC scores	Paired convolutional neural networks	250 patients (60% training, 40% testing)	Detection by paired convolutional neural networks identified more lesions than individual observers: • Sensitivity: 67–72% • False-positive rate: 0.48–1.69 errors per scan
Al'Aref 2017[19]	Accurate, automated identification of CAC score	Gradient boosting machine learning	35 281 patients (CONFIRM registry) (70% training, 30% testing)	AUC • CAC score 0: 0.84 • CAC score 1–100: 0.67 • CAC score 101–400 : 0.74 • CAC score >400: 0.85
Nakanishi 2017[20]	Retrospective analysis of the capability of ML-determined CAC, clinical data and CT variables vs. each individual factor in predicting coronary heart disease or cardiovascular death.	-	66 636 participants without cardiovascular disease from the Multi-Ethnic Study of Atherosclerosis (MESA)	AUC • ML (all variables): 0.85 • Clinical data only: 0.83 • CAC score only: 0.81 • CT variables only: 0.82
Durlak 2017[21]	Automated CAC labelling system vs. expert reader	Atlas-based feature approach and random forest classifier	40 patients	ICC: 0.99 Accuracy: 1.0 κ Run time: 10 s
Lossau (née Elss) 2019[22]	Use of ML to improve interpretability through reducing motion artefact by predicting motion direction.	CNN	19 clinical datasets	Motion direction error: 34.9 ± 1.21 Motion magnitude error: 1.86 ± 0.11 mm
Commandeur 2020[23]	Prospective analysis of the capability of ML-determined CAC score and other variables in predicting MI or cardiac death.	Extreme gradient boosting	1912 participants without cardiovascular disease	AUC • ML: 0.82 • ASCVD: 0.77 • CAC: 0.77
Al'Aref 2020[24]	ML model using CAC and clinical factors to improve prediction of obstructive CAD.	Boosted ensemble algorithm	35 281 patients (CONFIRM registry) (80% training, 20% testing)	AUC • ML: 0.77 • CAD consortium clinical score: 0.73 • CAC score: 0.87 • UDF score: 0.68
Głowacki 2020[25]	ML model prediction of obstructive CAD following CAC score.	Gradient boosting machine learning	435 patients	Sensitivity 100 ± 0.0% Specificity 69.8 ± 3.6%
Lee 2020[26]	Retrospective analysis to ascertain best ML algorithm to predict CAC score from clinical variables.	Binary logistic regression, CatBoost, and XGBoost algorithms	2133 participants without cardiovascular disease	AUC • XGBoost: 0.82 • Catboost: 0.75 • Binary logistic regression: 0.59

Testing includes validation. Statistics are per patient.
ML, machine learning; CAC score, coronary artery calcium score; CNN, convolutional neural networks; AUC, area under the curve; ASCVD, atherosclerotic cardiovascular disease risk algorithm; CAD, coronary artery disease; UDF score, updated Diamond–Forrester score; ICC, intraclass correlation coefficient.

Table 4 Summary of articles investigating the use of ML in cardiac CT determined plaque characterization

Study	Design and aim	Algorithm used	Population	Outcome
Wei 2014[27]	Retrospective, automated detection of non-calcified plaques, grouped by vessel diameter	Topological soft-gradient detection method	83 patients	AUC: 0.87 ± 0.01 Sensitivity: 70–90% False-positive rate: 1.39–3.16 per scan
Dey 2018[28]	Prospective, multicentre trial performing semi-automated quantification of calcified and non-calcified plaques, and plaque length and volume	Ensemble classification approach with LogitBoost and single-node decision trees	80 patients (90% training, 10% testing)	Information gain ratio • Low-density non-calcified plaques: 0.097 • Plaque length: 0.092 • Plaque volume: <0.001
Masuda 2019[29]	Retrospective comparison of ML-determined plaque characterization vs. median CT number	Extreme gradient boosting	78 patients	AUC • ML: 0.92 (95% CI: 0.86–0.92) • Median CT number: 0.83 (95% CI: 0.75–0.92)
Zreik 2019[30]	Retrospective, detection, characterization and assessment of stenosis	Multi-task recurrent convolutional neural network	163 patients (60% training, 40% testing)	Accuracy • Detection and characterization: 0.77 • Stenosis: 0.80
Al'Aref 2020[31]	Case-control study identifying culprit lesions with multiple models	Boosted ensemble algorithm	468 patients at high-risk of ACS (80% training, 20% testing)	AUC of best model: 0.77 (95% CI: 0.60–0.76)
Han 2020[32]	Retrospective cohort study identification of individuals at risk of rapid coronary plaque progression	Boosted ensemble classification (LogitBoost)	1083 patients who underwent serial CTs in the PARADIGM registry (70% training, 30% testing)	AUC: 0.83 (95% CI: 0.78–0.89)
Muscogiuri 2020[33]	Automated categorization to Coronary Artery Disease Reporting and Data System (CAD-RADS) guidance using three models	CNN	208 patients	Sensitivity: 47–82% Specificity: 58–91% Negative predictive value: 74–92% Positive predictive value: 46–69% Accuracy: 60–86% Classification time • ML: 104 s per read • Expert reader: 530 s per read
Tesche 2021[34]	Retrospective prognostication using clinical parameters and ML-derived plaque characteristics at 5-year follow-up	Boosted ensemble algorithm (RUSBoost)	361 patients with suspected CAD	AUC 0.96 Sensitivity 0.97 Specificity 0.86
Yang 2021[35]	Retrospective prognostication using clinical parameters and ML-derived plaque characteristics at 5-year follow-up	Boruta algorithm and hierarchical clustering	1013 vessels	AUC for low FFR of best model: 0.797 ($P <$ 0.001)

Testing includes validation. Statistics are per patient.
95% CI, 95% confidence interval; CNN: convolutional neural network; MACE, major adverse cardiovascular events; ML, machine learning; AUC, area under the curve; CAD, coronary artery disease.

have demonstrated CNN algorithms that can automatically segment the LA with 99% accuracy vs. expert reader,[58] and compartmentalize the LA into individual sub-sections using marginal space learning-based object segmentation with minimal error (*Table 7*).[56] Post-ablation recurrence of AF has a rate of ca. 45%; Firouzina *et al.*[60] successfully used random forest classifiers to identify

Table 5 Summary of articles investigating the use of ML in cardiac CT determined EAT

Study	Design and aim	Algorithm used	Population	Outcome
Rodrigues 2016[36]	Prospective, automatic segmentation of mediastinal and epicardial adipose tissue using several algorithms compared with manual segmentation	CNN, probabilistic models, and decision tree algorithms	20 patients	Random forest classification was superior Accuracy: 98.5% DSC for mediastinal and EAT: 0.98
Norlén 2016[37]	Automatic pericardial segmentation and epicardial adipose tissue quantification vs. expert readers	Multi-atlas technique and random forest classification combined into a Markov random field	30 examinations (SCAPIS study) (training 67%, testing 33%)	Pearson's correlation vs. two experts: $r > 0.998$ Segmentation time: 52 s
Rodrigues 2017[38]	Prediction of mediastinal and epicardial adipose tissue volumes vs. expert readers	Rotation forest algorithm using multilayer perceptron Regressor	50 examination images	Pearson's correlation: 0.988 Relative absolute error: 14.4% Root relative squared error 15.7%
Commandeur 2018[39]	Fully automated assessment of mediastinal and epicardial adipose tissue vs. expert readers	CNN	250 participants (80% training, 20% testing)	Pearson's correlation • EAT: 0.924 • Mediastinal adipose tissue: 0.945 DSC • EAT: 0.823 • Mediastinal adipose tissue: 0.905
Commandeur 2019[40]	Fully automated quantification and assessment of progression at follow-up of mediastinal and epicardial adipose tissue vs. expert readers	CNN with TensorFlow framework	850 participants (80% training, 20% testing)	Pearson's correlation vs. expert reader • Quantification: $r > 0.973$ • Progression at follow-up: $r = 0.905$ Quantification mean time: 1.57 s
Oikonomou 2019[41]	Prediction of cardiac risk by analysis of radiomic profile of coronary perivascular adipose tissue (three studies)	Random forest	312 patients	• Radiomic features linked to expression of inflammatory, fibrotic and vascularity genes • Fat radiomic profile provided superior MACE prediction at 5-year follow-up relative to traditional risk stratification • Fat radiomic profile elevated in patients with MI relative to matched controls
Chernina 2020[42]	Retrospective, automatic vs. semi-automatic vs. expert radiologist for acquisition of EAT volume	3D convolutional network	452 (78% training, 22% testing)	Pearson's correlation • ML vs. semi-automatic: $r > 0.95$ • ML vs. expert radiologists: $r > 0.98$
He 2000b[43]	Retrospective, simultaneous myocardial and pericardial fat quantification	3D deep attenuation U-Net (DAU-net)	422 patients with suspected CVD (testing)	Median DSC pericardial fat: 0.88 Median DSC myocardium: 0.96 Consistency with contour, ICC: 0.97; $P < 0.05$
He 2000a[44]	Retrospective, automatic vs. manual segmentation of epicardial adipose tissue	3D deep attenuation U-Net (DAU-net)	200 patients	Sensitivity: 0.91 Specificity: 0.95 ML median DSC pericardial fat: 0.93 Manual control median DSC pericardial fat: 0.92
Kroll 2021[45]	Retrospective comparison of CAC scores and pericardial fat in coronary calcium CT scans	Multi-resolution U-Net 3D network	1066 patients at intermediate risk of CAD (9% training, 91% testing)	Demonstrated automated adipose tissue analysis. Median DSC pericardium/muscle: 0.96

Testing includes validation. Statistics are per patient. Accuracy was defined in Rodrigues[36] as (true positive + true negative/total population). CNN, convolutional neural networks; DSC, dice similarity coefficient; EAT, epicardial adipose tissue; MACE, major adverse cardiovascular events; MI, myocardial infarction; ML, machine learning.

Table 6 Summary of articles investigating the use of ML, cardiac CT, and AS

Study	Design and aim	Algorithm used	Participants	Outcome
Grbic 2013[46]	Retrospective, automated prediction of aortic annulus perimeter and area	—	11	Accuracy: 1.30 ± 23 mm Predicted implant size error: 1.75 ± 40 mm Aortic annulus error: 1.32 mm 'errors in predicted implant deployment were of 1.74 ± 0.4 mm in average and 1.32 mm in aortic valve annulus region, which is almost three times lower than the average gap of 3 mm between consecutive implant sizes.'
Elattar 2014[47]	Automated segmentation of the aortic root	Connected component analysis and fuzzy classification	20	DSC • ML: 0.95 ± 0.03 • Expert reader: 0.95 ± 0.03 Mean error • ML: 0.74 ± 0.39 mm • Expert reader: 0.68 ± 0.34 mm Time • ML: 90 s Expert reader: 20 min
Liang 2017[48]	Automated reconstruction of the aortic valve	Neighbour-constrained segmentation	10	Mean discrepancy ML vs. expert reader: 1.57 mm
Al Abdullah 2018[49]	Automated identification of aortic valve landmarks	Randomized regression tree-based algorithm (colonial walk)	71	Mean localization error: 2.04 mm Inter-observer variability: 2.38 mm Time • ML: 12 mss • Expert reader: 4 min
Astudillo 2019[50]	Retrospective, automated prediction of aortic annulus perimeter and area	CNN	473 patients (75% training, 25% testing)	Difference between predicted values and device size selected: Area • ML: 3.3 ± 16.8 mm^2 • Expert reader: 1.3 ± 21.1 mm^2 Perimeter • ML: 0.6 ± 1.7 mm • Expert reader: 0.2 ± 2.5 mm The difference between manually obtained aortic annulus measurements and those produced by the automated method were comparable to intra-operator variability
Theriault-Lauzier 2020[51]	Automated location and orientation of the aortic valve annular plane	CNN	94 patients with severe AS	Relative measurement error • Annular area: 4.73 ± 5.32% Annular perimeter: 2.46 ± 2.94%
Agasthi 2021[52]	Retrospective, predictive modelling of 1-year life expectancy of TAVR candidates	Gradient boosting ML (caret R package)	1055	AUC 1 year: 0.72
Kang 2021[53]	Predictive modelling to diagnose AS using CT features of aortic valve calcium	Least absolute shrinkage and selection operator (LASSO), random forests, and eXtreme Gradient boosting (XGBoost)	Retrospective study of 408 patients (240 with and 168 without severe AS)	3/9 radiomics prediction models were successful in showing greater ability to distinguish AS. Differences for all models were not statistically significant ($P > 0.05$)
Maeda 2021[54]	Retrospective, predictive modelling of life-expectancy of TAVR candidates	Cox proportional hazard regression	388 (259	AUC 1 year: 0.79

Continued

Table 6 ***Continued***

Study	Design and aim	Algorithm used	Participants	Outcome
			training, 129 testing)	3 years: 0.76 5 years: 0.78
Shirakawa 2021[55]	Proof-of-concept automated precise segmentation from CT of cardiac structure in the pre-operative assessment of patients with HOCM	CNN	2	ML segmentation was ca. 36 faster

Testing includes validation. Statistics are per patient.
ML, machine learning, DSC, dice similarity coefficient; AUC, area under the curve; CNN, convolutional neural network; HOCM, hypertrophic obstructive cardiomyopathy.

Table 7 **Summary of articles investigating the use of ML, cardiac CT, and AF**

Study	Design and aim	Algorithm used	Population	Outcome
Zheng 2014[56]	Retrospective subsection segmentation of the left atrium	Marginal space learning-based object segmentation	687 datasets	Mean mesh error • Small volumes: 1.07 mm • Large volumes: 1.32 mm
Bratt 2019[57]	Retrospective prediction of AF using left atrial volume vs. expert reader	CNN (U-Net)	1000 patients undergoing routine CT thoraxes (50% training, 50% testing)	AUC: 0.77 (95% CI: 0.71–0.82) Age-adjusted relative risk: 2.9 Mean DSC • ML: 0.85 • Expert reader: 0.84
Chen 2020[58]	Retrospective detection and segmentation of the left atrium vs. expert reader	CNN (U-Net)	518 patients who underwent pulmonary vein ablation	Accuracy: 99.0% Sensitivity 99.3% Specificity: 98.7%
Liu 2020[59]	Retrospective prediction of post-ablation AF recurrence due to non-pulmonary vein triggers	CNN (U-Net) (ResNet34)	521 patients (73% training, 27% testing)	AUC: 0.88 $\pm$ 0.07 Accuracy: 88.6% $\pm$2.3 Sensitivity 75.0% $\pm$5.8 Specificity 95.7% $\pm$1.8
Firouznia 2021[60]	Retrospective prediction of post-ablation AF recurrence using morphological analysis of the left atrial myocardium and pulmonary veins	Random forest	203 patients	AUC: 0.87 (95% CI: 0.82–0.93)
Deepa 2021[61]	Prospective ML detection of epicardial fat within the left atrium	CNN	10 patients	Accuracy: 89.22% Sensitivity: 90.18% Specificity: 88.52%
Atta-Fosu 2021[62]	Retrospective investigation of left atrial shape differences and prediction of post-ablation AF recurrence	Gradient boosted classifier (XGBoost)	68 patients	AUC for shape features from the SOI: 0.67 AUC for clinical parameters: 0.71

Testing includes validation. Statistics are per patient.
AUC, area under the curve; AF, atrial fibrillation; CNN, convolutional neural network; DSC, dice similarity coefficient; ML, machine learning; SOI, shape of interest.

morphological traits on 3D fractal features to predict the risk of AF recurrence from pre-ablation contrast CTs (AUC: 0.87). This is likely because LA wall thickness and scarring depth that can be detected pre-procedure, relate to ablation success. Atta-Fosu *et al.*[62] employed a similar technique using Gradient boosted classifiers (XGBoost) and found a lower AUC for shape alone (0.67) that was similar when combined with clinical features (0.78). In addition, it has been reported that post-ablation AF recurrence secondary to non-PV triggers can also be predicted with a similarly high degree of performance (AUC: 0.88).[59] Given the utility of LA volumes measurements obtained by cardiac CT, it has been incorporated into a recently validated ATLAS score to predict AF recurrence after first PV isolation radiofrequency PV isolation ablation.[72] Indeed, the application of CNN algorithms to the measurement of LV volume on routine non-gated chest CT have been able to effectively predict AF.[59] Given the morbidity and mortality associated with undiagnosed paroxysmal AF and the increasing use of thoracic CT imaging this may be a worthwhile add-on.

Discussion and limitations

Given the black-box nature of commercial ML tools, we may not be able to fully analyse the reasoning behind the outputs of these complex models, and as such may not easily identify implicit biases within a given dataset or methodology. Algorithms lack context and causality for their predictions. This may be less of an issue for algorithms which aim to automate calcium measurements but would be very significant for example in predictive algorithms for AF status or neural networks to simulate device biomechanics for TAVR.

Candidate selection and accurate labelling for the training of models are the most crucial steps in the development of ML protocols. Disparities in these factors between studies may explain variability in results demonstrated in *Tables 2–7*. Utilizing large multicentre studies, such as Nakanishi *et al.*,[73] in predicting coronary heart disease events from CTs from the Multi-Ethnic Study of Atherosclerosis cohort, or Coenen *et al.*,[6] for assessing the diagnostic accuracy of CT-FFR$_{ML}$ within the MACHINE consortium, is a useful start in the optimization of models for a broader patient population and may account for labelling issues in training datasets. Reproducibility can also be hampered by a requirement for specific CT scanner capabilities, the use of distinct imaging protocols, and other methodological heterogeneity. Machine learning has already been applied to automate image quality assessment in CCTA studies in a reproducible manner, which may provide a tool to stratify clinical trials to the levels of image quality. Another challenge that is apparent from the findings of this review is the lack of standardization in metrics used to analyse outcomes (i.e. AUC, dice coefficients, or accuracy). Though the chosen metric is matched to the task it is undertaking, for example, AUC for classification or DC for segmentation, this hampers comparability. Many ML models exist to address the same task with varying metrics of performance and results, as evidenced by *Tables 2–7*. Approaches such as that undertaken by Lopes *et al.*,[74] who compared several ML models on a single large standardized dataset, need to increasingly be undertaken to provide more insights into an optimal methodology for diagnostic and prognostic reliability. With the introduction of a new datasets, the models will need to be continually retrained and in so doing new features may need to be accounted for.

Conclusion

Application of ML protocols to cardiac CT output has many benefits in automating time-consuming calculations, risk stratification and prognostication, and in pre-operative procedure planning across several pathologies including CAD, epicardial adiposity quantification, AF, and AS. Machine learning provides exciting advances in CCT- and CCTA-based calcium scoring and in near real-time analysis of flow-limiting lesions on CT-FFR. ML-CT-derived measurements and predictive prognostics may assist patient selection for radiofrequency ablation in patients with refractory AF. ML-CT may guide device selection and improve pre-procedural processes for TAVR candidates. Though far from replacing the bedside physician, efforts to incorporate these novel models into clinical practice may reduce time and resources while at the same time improving patient outcomes.

Lead author biography

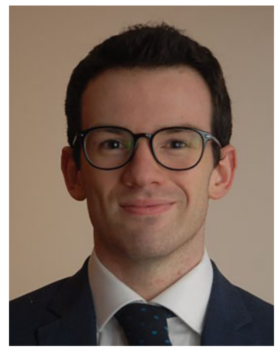

Dr Jonathan J. H. Bray is an Academic Junior Doctor and The Training Manager for the British Junior Cardiologists Association (BJCA) Starter committee. Jonathan intercalated in Physiological Sciences at the University of Bristol in 2016. He has published 17 peer-reviewed articles, given seven international or national presentations and been awarded almost £3000 as part of a number of awards and prizes. He is a solicited peer review of several high impact journals and contributes as an author to the Cochrane collaborative. He teaches three courses at Cardiff and Swansea University as Honorary Tutor and Research Fellow.

Acknowledgements

The authors would like to thank Biorender for the images used in the central schematic. No further data were obtained beyond that set out in the manuscript.

Conflict of interest: none declared.

References

1. Albrecht MH, De Cecco CN, Schoepf UJ, Spandorfer A, Eid M, De Santis D, Varga-Szemes A, van Assen M, von Knebel-Doeberitz PL, Tesche C, Puntmann VO, Nagel E, Vogl TJ, Nance JW. Dual-energy CT of the heart current and future status. *Eur J Radiol* 2018;**105**:110–118.
2. Chahal H, Levsky JM, Garcia MJ. Cardiac CT: present and future applications. *Heart* 2016;**102**:1840–1850.
3. Ronneberger O, Fischer P, Brox T. U-Net: convolutional networks for biomedical image segmentation. In International Conference on Medical Image Computing and Computer-Assisted Intervention. Cham: Springer; 2015. p234–241.
4. Schulz KF, Altman DG, Moher D, the CONSORT Group. CONSORT 2010 Statement: updated guidelines for reporting parallel group randomised trials. *BMC Med* 2010;**8**:18.
5. Itu L, Rapaka S, Passerini T, Georgescu B, Schwemmer C, Schoebinger M, Flohr T, Sharma P, Comaniciu D. A machine-learning approach for computation of fractional flow reserve from coronary computed tomography. *J Appl Physiol* 2016;**121**:42–52.
6. Coenen A, Kim YH, Kruk M, Tesche C, De Geer J, Kurata A, Lubbers ML, Daemen J, Itu L, Rapaka S, Sharma P, Schwemmer C, Persson A, Schoepf UJ, Kepka C, Hyun YD, Nieman K. Diagnostic accuracy of a machine-learning approach to coronary computed tomographic angiography–based fractional flow reserve: result from the MACHINE consortium. *Circ Cardiovasc Imaging* 2018;**11**:e007217.
7. Tesche C, De Cecco CN, Albrecht MH, Duguay TM, Bayer RR, Litwin SE, Steinberg DH, Schoepf UJ. Coronary CT angiography-derived fractional flow reserve. *Radiology* 2017;**285**:17–33.
8. Xu PP, Li JH, Zhou F, Jiang MD, Zhou CS, Lu MJ, Tang CX, Zhang XL, Yang L, Zhang YX, Wang YN, Zhang JY, Yu MM, Hou Y, Zheng MW, Zhang B, Zhang DM, Yi Y, Xu L, Hu XH, Liu H, Lu GM, Ni QQ, Zhang LJ. The influence of image quality on diagnostic performance of a machine learning–based fractional flow reserve derived from coronary CT angiography. *Eur Radiol* 2020;**30**:2525–2534.
9. Zreik M, van Hamersvelt RW, Khalili N, Wolterink JM, Voskuil M, Viergever MA, Leiner T, Išgum I. Deep learning analysis of coronary arteries in cardiac CT angiography for detection of patients requiring invasive coronary angiography. *IEEE Trans Med Imaging* 2020;**39**:1545–1557.

10. Baumann S, Hirt M, Schoepf UJ, Rutsch M, Tesche C, Renker M, Golden JW, Buss SJ, Becher T, Bojara W, Weiss C, Papavassiliu T, Akin I, Borggrefe M, Schoenberg SO, Haubenreisser H, Overhoff D, Lossnitzer D. Correlation of machine learning computed tomography-based fractional flow reserve with instantaneous wave free ratio to detect hemodynamically significant coronary stenosis. *Clin Res Cardiol* 2020;**109**: 735–745.
11. Lossnitzer D, Chandra L, Rutsch M, Becher T, Overhoff D, Janssen S, Weiss C, Borggrefe M, Akin I, Pfleger S, Baumann S. Additional value of machine-learning computed tomographic angiography-based fractional flow reserve compared to standard computed tomographic angiography. *J Clin Med* 2020;**9**:676.
12. Li Y, Qiu H, Hou Z, Zheng J, Li J, Yin Y, Gao R. Additional value of deep learning computed tomographic angiography-based fractional flow reserve in detecting coronary stenosis and predicting outcomes. *Acta Radiol* 2022;**63**:133–140.
13. Morais TC, Assunção AN Jr, Dantas Júnior RN, Silva CFGD, Paula CBD, Torres RA, Magalhães TA, Nomura CH, Ávila LFRD, Parga JR. Diagnostic performance of a machine learning-based CT-derived FFR in detecting flow-limiting stenosis. *Arq Bras Cardiol* 2021;**116**:1091–1098.
14. Tesche C, Otani K, De Cecco CN, Coenen A, De Geer J, Kruk M, Kim YH, Albrecht MH, Baumann S, Renker M, Bayer RR. Influence of coronary calcium on diagnostic performance of machine learning CT-FFR: results from MACHINE registry. *JACC Cardiovasc Imaging* 2020;**13**:760–770.
15. Renker M, Baumann S, Hamm CW, Tesche C, Kim WK, Savage RH, Coenen A, Nieman K, De Geer J, Persson A, Kruk M, Kepka C, Yang DH, Schoepf UJ. Influence of coronary stenosis location on diagnostic performance of machine learning-based fractional flow reserve from CT angiography. *J Cardiovasc Comput Tomogr* 2021;**15**:492–498.
16. Išgum I, Rutten A, Prokop M, van Ginneken B. Detection of coronary calcifications from computed tomography scans for automated risk assessment of coronary artery disease. *Med Phys* 2007;**34**:1450–1461.
17. Shahzad R, van Walsum T, Schaap M, Rossi A, Klein S, Weustink AC, de Feyter PJ, van Vliet LJ, Niessen WJ. Vessel specific coronary artery calcium scoring: an automatic system. *Acad Radiol* 2013;**20**:1–9.
18. Wolterink JM, Leiner T, de Vos BD, van Hamersvelt RW, Viergever MA, Išgum I. Automatic coronary artery calcium scoring in cardiac CT angiography using paired convolutional neural networks. *Med Image Anal* 2016;**34**:123–136.
19. AlAref S, Anchouche K, Wang H, Kolli K, Berman D, Callister T, DeLago A, Hadamitzky M, Hausleiter J, Al-Mallah M, Budoff M, Kaufmann P, Raff G, Chinnaiyan K, Cademartiri F, Maffei E, Villines TC, Kim Y-J, Jonathon Leipsic G, Pontone G, Andreini D, Marques H, Rubinshtein R, Achenbach S, Shaw LJ, Dunning AM, Gomez M, Hindoyan N, Lin FY, Pena JM, Min JK, Jones EC. Utilization of readily available clinical characteristics for the estimation of the coronary artery calcium score. *Clin Cardiol* 2017;**40**:8.
20. Nakanishi R, Slomka P, Betancur J, Blaha MJ, Nasir K, Miedema MD, Rumberger JA, Gransar H, Shaw LJ, Rozanski A, Budoff MJ. Machine learning adds to standard clinical & CAC assessments in predicting 10-year coronary heart disease & cardiovascular disease deaths: insight from the coronary artery calcium consortium of 66,636 patients. *Circulation* 2017;**136**:A15137.
21. Durlak F, Wels M, Schwemmer C, Sühling M, Steidl S, Maier A. Growing a random forest with fuzzy spatial features for fully automatic artery-specific coronary calcium scoring. In: Wang Q, Shi Y, Suk HI, Suzuki K, eds. *Machine Learning in Medical Imaging. MLMI 2017. Lecture Notes in Computer Science*. vol. 10541. Cham: Springer; 2017. p27–35. doi:10.1007/978-3-319-67389-9_4.
22. Lossau T, Nickisch H, Wissel T, Bippus R, Schmitt H, Morlock M, Grass M. Motion estimation and correction in cardiac CT angiography images using convolutional neural networks. *Comput Med Imaging Graph* 2019;**76**:101640.
23. Commandeur F, Slomka PJ, Goeller M, Chen X, Cadet S, Razipour A, McElhinney P, Gransar H, Cantu S, Miller RJ, Rozanski A, Achenbach S, Tamarappoo BK, Berman DS, Dey D. Machine learning to predict the long-term risk of myocardial infarction and cardiac death based on clinical risk, coronary calcium, and epicardial adipose tissue: a prospective study. *Cardiovasc Res* 2020;**116**:2216–2225.
24. Al'Aref SJ, Maliakal G, Singh G, van Rosendael AR, Ma X, Xu Z, Alawamlh OAH, Lee B, Pandey M, Achenbach S, Al-Mallah MH, Andreini D, Bax JJ, Berman DS, Budoff MJ, Cademartiri F, Callister TQ, Chang H-J, Chinnaiyan K, Chow BJW, Cury RC, DeLago A, Feuchtner G, Hadamitzky M, Hausleiter J, Kaufmann PA, Kim Y-J, Leipsic JA, Maffei E, Marques H, Gonçalves PA, Pontone G, Raff GL, Rubinshtein R, Villines TC, Gransar H, Lu Y, Jones EC, Peña JM, Lin FY, Min JK, Shaw LJ. Machine learning of clinical variables and coronary artery calcium scoring for the prediction of obstructive coronary artery disease on coronary computed tomography angiography: analysis from the CONFIRM registry. *Eur Heart J* 2020;**41**:359–367.
25. Glowacki J, Krysinski M, Czaja-Ziolkowska M, Wasilewski J. Machine learning-based algorithm enables the exclusion of obstructive coronary artery disease in the patients who underwent oronary artery calcium scoring. *Acad Radiol* 2020;**27**: 1416–1421.
26. Lee J, Lim JS, Chu Y, Lee CH, Ryu OH, Choi HH, Park YS, Kim C. Prediction of coronary artery calcium score using machine learning in a healthy population. *J Pers Med* 2020;**10**:1–10.
27. Wei J, Zhou C, Chan HP, Chughtai A, Agarwal P, Kuriakose J, Hadjiiski L, Patel S, Kazerooni E. Computerized detection of noncalcified plaques in coronary CT angiography: evaluation of topological soft gradient prescreening method and luminal analysis. *Med Phys* 2014;**41**:081901.
28. Dey D, Gaur S, Ovrehus KA, Slomka PJ, Betancur J, Goeller M, Hell MM, Gransar H, Berman DS, Achenbach S, Botker HE, Jensen JM, Lassen JF, Norgaard BL. Integrated prediction of lesion-specific ischaemia from quantitative coronary CT angiography using machine learning: a multicentre study. *Eur Radiol* 2018;**28**:2655–2664.
29. Masuda T, Nakaura T, Funama Y, Okimoto T, Sato T, Higaki T, Noda N, Imada N, Baba Y, Awai K. Machine-learning integration of CT histogram analysis to evaluate the composition of atherosclerotic plaques: validation with IB-IVUS. *J Cardiovasc Comput Tomogr* 2019;**13**:163–169.
30. Zreik M, Van Hamersvelt RW, Wolterink JM, Leiner T, Viergever MA, Isgum I. A recurrent CNN for automatic detection and classification of coronary artery plaque and stenosis in coronary CT angiography. *IEEE Trans Med Imaging* 2019;**38**: 1588–1598.
31. Al'Aref SJ, Singh G, Choi JW, Xu Z, Maliakal G, van Rosendael AR, Lee BC, Fatima Z, Andreini D, Bax JJ, Cademartiri F, Chinnaiyan K, Chow BJW, Conte E, Cury RC, Feuchtner G, Hadamitzky M, Kim Y-J, Lee S-E, Leipsic JA, Maffei E, Marques H, Plank F, Pontone G, Raff GL, Villines TC, Weirich HG, Cho I, Danad I, Han D, Heo R, Lee JH, Rizvi A, Stuijfzand WJ, Gransar H, Lu Y, Sung JM, Park H-B, Berman DS, Budoff MJ, Samady H, Stone PH, Virmani R, Narula J, Chang H-J, Lin FY, Baskaran L, Shaw LJ, Min JK. A boosted ensemble algorithm for determination of plaque stability in high-risk patients on coronary CTA. *JACC Cardiovasc Imaging* 2020;**13**:2162–2173.
32. Han D, Kolli KK, Al'Aref SJ, Baskaran L, van Rosendael AR, Gransar H, Andreini D, Budoff MJ, Cademartiri F, Chinnaiyan K, Choi JH. Machine learning framework to identify individuals at risk of rapid progression of coronary atherosclerosis: from the PARADIGM registry. *J Am Heart Assoc* 2020;**9**:e013958.
33. Muscogiuri G, Chiesa M, Trotta M, Gatti M, Palmisano V, Dell'Aversana S, Baessato F, Cavaliere A, Cicala G, Loffreno A, Rizzon G, Guglielmo M, Baggiano A, Fusini L, Saba L, Andreini D, Pepi M, Rabbat MG, Guaricci AI, De Cecco CN, Colombo G, Pontone G. Performance of a deep learning algorithm for the evaluation of CAD-RADS classification with CCTA. *Atherosclerosis* 2020;**294**:25–32.
34. Tesche C, Bauer MJ, Baquet M, Hedels B, Straube F, Hartl S, Gray HN, Jochheim D, Aschauer T, Rogowski S, Schoepf UJ, Massberg S, Hoffmann E, Ebersberger U. Improved long-term prognostic value of coronary CT angiography-derived plaque measures and clinical parameters on adverse cardiac outcome using machine learning. *Eur Radiol* 2021;**31**:486–493.
35. Yang S, Koo BK, Hoshino M, Lee JM, Murai T, Park J, Zhang J, Hwang D, Shin E-S, Doh J-H, Nam C-W, Wang J, Chen S, Tanaka N, Matsuo H, Akasaka T, Choi G, Petersen K, Chang H-J, Kakuta T, Narula J. CT angiographic and plaque predictors of functionally significant coronary disease and outcome using machine learning. *JACC Cardiovasc Imaging* 2021;**14**:629–641.
36. Rodrigues ÉO, Morais FFC, Morais NAOS, Conci LS, Neto LV, Conci A. A novel approach for the automated segmentation and volume quantification of cardiac fats on computed tomography. *Comput Methods Programs Biomed* 2016;**123**:109–128.
37. Norlén A, Alvén J, Molnar D, Enqvist O, Norrlund RR, Brandberg J, Bergström G, Kahl F. Automatic pericardium segmentation and quantification of epicardial fat from computed tomography angiography. *J Med Imaging* 2016;**3**:034003.
38. Rodrigues ÉO, Pinheiro VHA, Liatsis P, Conci A. Machine learning in the prediction of cardiac epicardial and mediastinal fat volumes. *Comput Biol Med* 2017;**89**:520–529.
39. Commandeur F, Goeller M, Betancur J, Cadet S, Doris M, Chen X, Berman DS, Slomka PJ, Tamarappoo BK, Dey D. Deep learning for quantification of epicardial and thoracic adipose tissue from non-contrast CT. *IEEE Trans Med Imaging* 2018; **37**:1835–1846.
40. Commandeur F, Goeller M, Razipour A, Cadet S, Hell MM, Kwiecinski J, Chen X, Chang HJ, Marwan M, Achenbach S, Berman DS, Slomka PJ, Tamarappoo BK, Dey D. Fully automated CT quantification of epicardial adipose tissue by deep learning: a multicenter study. *Radiol Artif Intell* 2019;**1**:e190045.
41. Oikonomou EK, Williams MC, Kotanidis CP, Desai MY, Marwan M, Antonopoulos AS, Thomas KE, Thomas S, Akoumianakis I, Fan LM, Kesavan S, Herdman L, Alashi A, Centeno EH, Lyasheva M, Griffin BP, Flamm SD, Shirodaria C, Sabharwal N, Kelion A, Dweck MR, Van Beek EJR, Deanfield J, Hopewell JC, Neubauer S, Channon KM, Achenbach S, Newby DE, Antoniades C. A novel machine learning-derived radiotranscriptomic signature of perivascular fat improves cardiac risk prediction using coronary CT angiography. *Eur Heart J* 2019;**40**:3529–3543.
42. Chernina VY, Pisov ME, Belyaev MG, Bekk IV, Zamyatina KA, Korb TA, Aleshina OO, Shukina EA, Solovev AV, Skvortsov RA, Filatova DA, Sitdikov DI, Chesnokova AO, Morozov SP, Gombolevsky VA. Epicardial fat tissue volumetry: comparison of semiautomatic measurement and the machine learning algorithm. *Kardiologiia* 2020;**60**: 46–54.

43. He X, Guo BJ, Lei Y, Wang T, Curran WJ, Liu T, Zhang LJ, Yang X. Automatic quantification of myocardium and pericardial fat from coronary computed tomography angiography: a multicenter study. *Eur Radiol* 2021;**31**:3826–3836.
44. He X, Guo BJ, Lei Y, Wang T, Fu Y, Curran WJ, Zhang LJ, Liu T, Yang X. Automatic segmentation and quantification of epicardial adipose tissue from coronary computed tomography angiography. *Phys Med Biol* 2020;**65**:095012.
45. Kroll L, Nassenstein K, Jochims M, Koitka S, Nensa F. Assessing the role of pericardial fat as a biomarker connected to coronary calcification—a deep learning based approach using fully automated body composition analysis. *J Clin Med* 2021;**10**:356.
46. Grbic S, Mansi T, Ionasec R, Voigt I, Houle H, John M, Schoebinger M, Navab N, Comaniciu D. Image-based computational models for TAVI planning: from CT images to implant deployment. *Med Image Comput Comput Assist Interv* 2013;**16**: 395–402.
47. Elattar MA, Wiegerinck EM, Planken RN, vanbavel E, van Assen HC, Baan J, Marquering HA. Automatic segmentation of the aortic root in CT angiography of candidate patients for transcatheter aortic valve implantation. *Med Biol Eng Comput* 2014;**52**:611–618.
48. Liang L, Kong F, Martin C, Pham T, Wang Q, Duncan J, Sun W. Machine learning–based 3-D geometry reconstruction and modeling of aortic valve deformation using 3-D computed tomography images. *Int J Numer Method Biomed Eng* 2017;**33**:e2827.
49. Al WA, Jung HY, Yun ID, Jang Y, Park H-B, Chang H-J. Automatic aortic valve landmark localization in coronary CT angiography using colonial walk. *PLOS ONE* 2018; **13**:e0200317.
50. Astudillo P, Mortier P, Bosmans J, De Backer O, De Jaegere P, De Beule M, Dambre J. Enabling automated device size selection for transcatheter aortic valve implantation. *J Interv Cardiol* 2019;**2019**:1–7.
51. Theriault-Lauzier P, Alsosaimi H, Mousavi N, Buithieu J, Spaziano M, Martucci G, Brophy J, Piazza N. Recursive multiresolution convolutional neural networks for 3D aortic valve annulus planimetry. *Int J Comput Assist Radiol Surg* 2020;**15**:577–588.
52. Agasthi P, Ashraf H, Pujari SH, Girardo ME, Tseng A, Mookadam F, Venepally NR, Buras M, Khetarpal BK, Allam M, Eleid MF, Greason KL, Beohar N, Siegel RJ, Sweeney J, Fortuin FD, Holmes DR, Arsanjani R. Artificial intelligence trumps TAVI2-SCORE and CoreValve score in predicting 1-year mortality post-transcatheter aortic valve replacement. *Cardiovasc Revascularization Med* 2021;**24**: 33–41.
53. Kang N, Suh YJ, Han K, Kim Y, Choi BW. Performance of prediction models for diagnosing severe aortic stenosis based on aortic valve calcium on cardiac computed tomography: incorporation of radiomics and machine learning. *KJR* 2021;**22**:334.
54. Maeda K, Kuratani T, Pak K, Shimamura K, Mizote I, Miyagawa S, Toda K, Sakata Y, Sawa Y. Development of a new risk model for a prognostic prediction after transcatheter aortic valve replacement. *Gen Thorac Cardiovasc Surg* 2021;**69**:44–50.
55. Shirakawa T, Koyama Y, Shibata R, Fukui S, Tatsuoka M, Yoshitatsu M, Toda K, Fukuda I, Sawa Y. Automated heart segmentation using a convolutional neural network accelerates 3D model creation for cardiac surgery. *Eur Heart J Cardiovasc Imaging* 2021;**22**:356–353.
56. Zheng Y, Yang D, John M, Comaniciu D. Multi-part modeling and segmentation of left atrium in C-arm CT for image-guided ablation of atrial fibrillation. *IEEE Trans Med Imaging* 2014;**33**:318–331.
57. Bratt A, Guenther Z, Hahn LD, Kadoch M, Adams PL, Leung AN, Guo HH. Left atrial volume as a biomarker of atrial fibrillation at routine chest CT: deep learning approach. *Radiol Cardiothorac Imaging* 2019;**1**:e190057.
58. Chen HH, Liu CM, Chang SL, Chang PYC, Chen WS, Pan YM, Fang ST, Zhan SQ, Chuang CM, Lin YJ, Kuo L, Wu M-H, Chen C-K, Chang Y-Y, Shiu Y-C, Chen S-A, Lu HH-S. Automated extraction of left atrial volumes from two-dimensional computer tomography images using a deep learning technique. *Int J Cardiol* 2020;**316**: 272–278.
59. Liu CM, Chang SL, Chen HH, Chen WS, Lin YJ, Lo LW, Hu YF, Chung FP, Chao TF, Tuan TC, Liao JN. The clinical application of the deep learning technique for predicting trigger origins in patients with paroxysmal atrial fibrillation with catheter ablation. *Circ Arrhythm Electrophysiol* 2020;**13**:e008518.
60. Firouznia M, Feeny AK, LaBarbera MA, McHale M, Cantlay C, Kalfas N, Schoenhagen P, Saliba W, Tchou P, Barnard J, Chung MK, Madabhushi A. Machine learning–derived fractal features of shape and texture of the left atrium and pulmonary veins from cardiac computed tomography scans are associated with risk of recurrence of atrial fibrillation postablation. *Circ Arrhythm Electrophysiol* 2021;**14**:e009265.
61. Deepa D, Singh Y, Wang MC, Hu W. An automated method for detecting atrial fat using convolutional neural network. *Proc Inst Mech Eng H: J Eng Med* 2021;**235**: 1329–1334.
62. Atta-Fosu T, LaBarbera M, Ghose S, Schoenhagen P, Saliba W, Tchou PJ, Lindsay BD, Desai MY, Kwon D, Chung MK, Madabhushi A. A new machine learning approach for predicting likelihood of recurrence following ablation for atrial fibrillation from CT. *BMC Med Imaging* 2021;**21**:45.
63. Hewitt N, Dimmock P, Long J. *HeartFlow FFRCT for estimating fractional flow reserve from coronary CT angiography*. United Kingdom: National Institute for Health and Care Excellence (NICE) [Internet]; 2021.
64. Writing Committee Members, Gulati M, Levy PD, Mukherjee D, Amsterdam E, Bhatt DL, Birtcher KK, Blankstein R, Boyd J, Bullock-Palmer RP, Conejo T, Diercks DB, Gentile F, Greenwood JP, Hess EP, Hollenberg SM, Jaber WA, Jneid H, Joglar JA, Morrow DA, O'Connor RE, Ross MA, Shaw LJ. 2021 AHA/ACC/ASE/CHEST/SAEM/SCCT/SCMR guideline for the evaluation and diagnosis of chest pain: a report of the American College of Cardiology/American Heart Association Joint Committee on Clinical Practice Guidelines. *J Am Coll Cardiol* 2021;**78**:e187–e285.
65. Windecker S, Neumann FJ, Jüni P, Sousa-Uva M, Falk V. Considerations for the choice between coronary artery bypass grafting and percutaneous coronary intervention as revascularization strategies in major categories of patients with stable multivessel coronary artery disease: an accompanying article of the task force of the 2018 ESC/EACTS guidelines on myocardial revascularization. *Eur Heart J* 2019; **40**:204–212.
66. Joshi PH, Patel B, Blaha MJ, Berry JD, Blankstein R, Budoff MJ, Wong N, Agatston A, Blumenthal RS, Nasir K. Coronary artery calcium predicts cardiovascular events in participants with a low lifetime risk of cardiovascular disease: the Multi-Ethnic Study of Atherosclerosis (MESA). *Atherosclerosis* 2016;**246**:367–373.
67. Budoff MJ, Gul KM. Expert review on coronary calcium. *Vasc Health Risk Manag* 2008;**4**:315–324.
68. Neves PO, Andrade J, Monção H. Coronary artery calcium score: current status. *Radiol Bras* 2017;**50**:182–189.
69. Guglielmo M, Lin A, Dey D, Baggiano A, Fusini L, Muscogiuri G, Pontone G. Epicardial fat and coronary artery disease: role of cardiac imaging. *Atherosclerosis* 2021;**321**: 30–38.
70. Mack MJ, Leon MB, Thourani VH, Makkar R, Kodali SK, Russo M, Kapadia SR, Malaisrie SC, Cohen DJ, Pibarot P, Leipsic J, Hahn RT, Blanke P, Williams MR, McCabe JM, Brown DL, Babaliaros V, Goldman S, Szeto WY, Genereux P, Pershad A, Pocock SJ, Alu MC, Webb JG, Smith CR. Transcatheter aortic-valve replacement with a balloon-expandable valve in low-risk patients. *N Engl J Med* 2019; **380**:1695–1705.
71. Salgado RA, Leipsic JA, Shivalkar B, Ardies L, Van Herck PL, Op de Beeck BJ, Vrints C, Rodrigus I, Parizel PM, Bosmans J. Preprocedural CT evaluation of transcatheter aortic valve replacement: what the radiologist needs to know. *Radiographics* 2014;**34**: 1491–1514.
72. Mesquita J, Ferreira AM, Cavaco D, Moscoso Costa F, Carmo P, Marques H, Morgado F, Mendes M, Adragão P. Development and validation of a risk score for predicting atrial fibrillation recurrence after a first catheter ablation procedure–ATLAS score. *Europace* 2018;**20**:f428–f435.
73. Nakanishi R, Dey D, Commandeur F, Slomka P, Betancur J, Gransar H, Dailing C, Osawa K, Berman D, Budoff M. Machine learning in predicting coronary heart disease and cardiovascular disease events: results from the multi-ethnic study of atherosclerosis (mesa). *J Am Coll Cardiol* 2018;**71**:A1483.
74. Lopes RR, van Mourik MS, Schaft EV, Ramos LA, Baan J Jr, Vendrik J, de Mol BAJM, Vis MM, Marquering HA. Value of machine learning in predicting TAVI outcomes. *Neth Heart J* 2019;**27**:443–450.